CONF-790538--9
79-83

PROPERTIES OF SINGLE CRYSTAL BETA"-ALUMINAS

J. B. BATES, G. M. BROWN,++ T. KANEDA,+ W. E. BRUNDAGE, J. C. WANG, and HERBERT ENGSTROM

Solid State and Chemistry Divisions, Oak Ridge National Laboratory, Oak Ridge, Tennessee 37830

ABSTRACT

Large single crystals of sodium beta"-alumina were grown by slow evaporation of Na_2O at 1690°C from a mixture of Na_2CO_3, MgO, and Al_2O_3. Polarized Raman measurements were made on the Naβ" single crystals and on single crystals of Li, K, Rb, and Agβ" prepared by ion exchange of Naβ". The low frequency Raman spectra of Na, K, Rb, and Agβ" contained four or more bands due to vibrations of the mobile cations. These results were analyzed by assuming the spectra to be due to the normal modes of a defect cluster consisting of a cation vacancy surrounded by three cations. From model calculations, the Raman band of Naβ" at 33 cm^{-1} is assigned to the attempt mode for diffusion of Na^+ ions. The structure of a Agβ" single crystal was investigated by neutron diffraction, and 20% of the Ag^+ ion sites were found to be vacant.

---

*Research sponsored by the Division of Materials Sciences, U. S. Department of Energy under contract W-7405-eng-26 with Union Carbide Corporation.

+Guest scientist on leave from Fuji Photo Film Co., Tokyo, Japan.

++Chemistry Division, ORNL.

INTRODUCTION

Sodium beta"-alumina (Naβ") is an important solid electrolyte material because of its high ionic conductivity: It has been reported [1] that the conductivity of Naβ" is several times larger than that of Naβ over a large temperature range. However, in contrast to the case of the beta-aluminas, many physical properties of the beta"-aluminas remain unknown because of the lack of single crystals of sufficient size and quality required by various experimental techniques. Recently we have been able to grow relatively large single crystals of Naβ". Studies of this material and of the Li, K, Rb, and Ag analogues by a variety of techniques have been initiated. In this paper, we survey the results of some of these studies. We will also discuss the results of our model calculations which were made in order to interpret the Raman scattering from Naβ" as well as to understand the conduction mechanism in this material.

CRYSTAL GROWTH, COMPOSITION, AND CONDUCTIVITY

Single crystals of Naβ"-alumina were grown by slow evaporation of Na_2O from a mixture consisting of 35 wt.% Na_2CO_3, 3 wt.% MgO, and 62 wt.% Al_2O_3 [2]. A platinum crucible was filled with the powdered mixture and tightly covered with a platinum lid having a small hole (~1 mm) in the center. The crucible was heated in a platinum resistance furnace at 1150°C for 10 h in order to convert the Na_2CO_3 to Na_2O. The temperature was then raised to 1690°C and held at this point for 24 to 72 h . After slowly cooling to room temperature, single crystals as large as 1.5 x 1 x 0.5 cm, with the short dimension parallel to the c-axis, were found on top of a thick section of hard, sintered material in the crucible. Chemical analyses of single crystals for Na, Mg, and Al gave the composition, $Na_{1.76}Mg_{0.60}Al_{10.35}O_{17}$ or 0.85 Na_2O· 6 MgO·5 Al_2O_3, where the oxygen content was assumed to be that required for charge compensation of the Na, Mg, and Al. This composition is close to that reported by Roth et al [3].

Weissenburg X-ray photographs of single crystals taken from each of several boules showed the pattern expected for Naβ"[4], and the lattice constants determined from these data, a_0 = 5.623 Å and c_0 = 33.591 Å, agree within experimental error with those determined from a recent neutron diffraction structure investigation of Naβ" [5]. Single crystals of Li, K, Rb, and Agβ" were prepared by ion exchange in the appropriate molten nitrate. A crystal of $^6Li\beta$" was prepared from a melt of $^6LiNO_3$ (95% $^6Li^+$).

The conductivity of a Naβ" single crystal with gold blocking electrodes was measured using a pulsed technique [6]. The sample was heated under vacuum for 2 h at 420°C, and the conductivity was measured under vacuum from 25 to 400°C.

The results of the conductivity measurements are shown in Fig. 1. These data differ in two major ways from those reported in Weber's earlier study [1]. First, the conductivity of our sample is (at room temperature) about one-fifth of that measured by Weber [1], and, second, our conductivity values followed Arrhenius behavior over the temperature range of the measurements, whereas the graph of Weber's log σT vs $1/T$ data was curved. The solid line in Fig. 1 represents the result of a least squares fit of the data to log σT vs $1/T$, and the activation energy from the slope of this line is 0.180 ± 0.003 eV. The cause of the difference between the conductivity of our single crystals of Naβ" and that of Weber's sample is not presently known, but it is reasonable to assume that it is due to some small difference in sample composition.

NEUTRON DIFFRACTION RESULTS

The structure of beta"-alumina was first determined by Bettman and Peters [4] from x-ray diffraction studies of magnesia stabilized single crystals. The primitive lattice is rhombohedral and belongs to the space group $R\bar{3}m$ (D^5_{3d}). In the ideal structure represented by the formula unit, $Na_2O \cdot MgO \cdot 5\ Al_2O_3$, there are six Na^+ ions in the triply primitive hexagonal cell (two in the primitive cell) located on the 6c sites (C_{3v} point symmetry). More recently Reidinger, LaPlaca, and Roth [5] investigated the structure of Naβ" using neutron diffraction. In the refinement of the structure, they placed the Na^+ ions in the 18h positions (C_s point symmetry) near the 6c sites with a total occupancy of 0.88 for each 6c site. Thus, the crystal contains 12% fewer Na^+ ions than the ideal structure. Because each cation may occupy one of three equivalent 18h sites related by a three-fold rotation about the 6c position, the cation sublattice is disordered.

The specimen of Agβ" alumina used in our diffraction experiments was approximately a rectangular parallelepiped with dimensions 1.1 x 6.0 x 4.7 mm (weight 114 mg). It was found by preliminary X-ray precession photography to be a single crystal of good quality having the symmetry of space group $R\bar{3}m$. The unit cell dimensions for the triply primitive hexagonal cell,

determined by the method of least squares from the second moments of 2θ scans of 21 reflections in the 2θ range to 50°, are given in Table I. Standard procedures were used to collect and make a preliminary reduction of intensity data for 664 independent neutron reflections. The preliminary processing included the application of absorption corrections.

Least-squares refinement of the structure of Agβ" alumina was started using the fractional coordinates furnished by Reidinger [5] for the isomorphous Naβ"-alumina.

At present, the structure has been refined to a discrepancy index R(F) of 0.045, using an isotropic extinction parameter [7]. Only a few reflections are greatly affected by extinction, though the largest correction factor on $\underline{F}_o^2$ is 2.69.

In the refinement process, it was found that the distribution of Ag^+ ions is better described with use of the 6c sites with 0.80 fractional occupancy rather than with use of the 18h sites used in the Reidinger description of the Naβ" structure [5]. The higher degree of disorder implied by the use of the 18h sites appears to be required in the model for Naβ" alumina in order to account for the considerably greater degree of smearing out of the Na^+ ion distribution as compared with that of the Ag^+ ion in Agβ". The contrast between the two distributions is also clearly shown by the comparison of the anisotropic thermal parameters $\underline{U}_{11}$, $\underline{U}_{22}$, and $\underline{U}_{33}$ for Na^+ and Ag^+ given in Table I. These differences imply a much tighter binding of Ag^+ compared to Na^+ in beta"-alumina, which is consistent with the result that Naβ" is a much better conductor than Agβ" [8].

A stereoscopic drawing of the Agβ" lattice is given in Fig. 2. The drawing includes the central two-thirds of two adjacent unit cells. The Ag^+ ions are displaced only ± 0.097 Å from the plane of the O(5) atoms, whereas in the Naβ" alumina the Na^+ ions are displaced by ± 0.181 Å from this plane [5]. Shifts of other atoms between the two structures are much smaller. The fractional occupancy of Mg^{2+} in the Al(2) sites, assuming full occupancy of the sites by Al^{3+} and Mg^{2+} together, is 0.34, in agreement with the corresponding result found for Naβ" alumina [5].

RAMAN SCATTERING AND MODEL CALCULATIONS

Raman scattering from beta"-aluminas was investigated for the primary purpose of identifying the attempt frequency for ion transport. The spectrometer and experimental techniques used for these measurements have been described elsewhere [9]. The 476.5 nm line of an argon laser operating with an output power of 600 mW was the excitation source in most measurements. Measurements were made at 15 and 300 K for all samples. The scattering geometry was defined by a set of orthogonal laboratory axes denoted by a, a', and c, where c is parallel to the crystallographic c-axis. The orientation of a and a' with respect to the crystallographic a-axis was not determined.

A comparison of the Raman scattering from Naβ and Naβ" below 250 cm^{-1} illustrated in Fig. 3 shows marked differences. The sharp band at 111 cm^{-1} in the Naβ" spectrum is due to an E_g phonon of the spinel block and corresponds to the pair of E_{1g}-E_{2g} phonon modes of Naβ seen at 117 and 110 cm^{-1}, respectively [10]. The remaining features in Fig. 3 are due to vibrations of the Na^+ ions in the respective materials. For Naβ, only a single broad band centered at ~63 cm^{-1} can definitely be ascribed to Na^+ vibrations, whereas, for Naβ", five or six bands, observed in different polarizations (see below), are assigned to mobile cation vibrations.

Raman spectra of Na, K, and Agβ" measured at 15 K in the region below 250 cm^{-1} for (a'a') polarization are shown in Fig. 4. The sharp band which appears at 111 cm^{-1} for Naβ", 116 cm^{-1} for Kβ", and at 109 cm^{-1} for Agβ" is due to an E_g phonon of the spinel block as noted above. The significantly larger width of the Kβ" phonon peak compared to that of Naβ" or Agβ" may be caused by overlap of this feature with a band due to a mode of the K^+ ions. Polarized Raman spectra of Liβ" in the region below 250 cm^{-1} contained only the E_g phonon peak at 110 cm^{-1}. We therefore attributed the remaining bands in Fig. 4 to vibrations of the mobile cations in the respective β"-aluminas. Just as we reported previously for the case of Liβ-alumina [9], Raman bands due to Li^+ modes in Liβ" were found in a much higher energy region (between 375 and 475 cm^{-1}) than expected based on the frequencies observed for Naβ". The frequencies of the Raman bands assigned to mobile cation vibrations are listed in Table II. The 22 cm^{-1} band of Agβ" not shown in Fig. 4 was seen only in samples of good optical quality with low background scattering.

We have made model calculations similar to those for the beta-aluminas [11] in order to understand the Raman scattering from the mobile cations and to study the conduction mechanism of the beta"-aluminas [12]. The potential energy model included Coulomb, short-range repulsive, and polarization energy terms. Starting from the ideal structure of Naβ" with all 6c Na^+ sites occupied, a Na^+ ion was removed from the crystal, and 13 Na^+ ions near the vacant site were allowed to relax so as to minimize the total potential energy of the system.

The calculated minimum energy configuration of the ions is illustrated in Fig. 5. This figure shows the O^{2-} ions in the conducting layer, the calculated positions of the Na^+ ions, which are displaced alternately above and below the plane of the O^{2-} ions, and the vacant sodium site. The three Na^+ ions surrounding a vacancy relax inward toward the vacancy, and the surrounding cations relax away from their ideal positions as shown in the figure. This result explains why, from the neutron diffraction data [5], all of the Na^+ ions were found to be located on the 18h positions near the 6c sites. The C_{3v} symmetry at a vacant site may or may not be preserved depending on the vacancy-ion distance. Our calculations showed that the most stable configuration above 0 K has one vacancy-cation distance slightly larger than the other two. The symmetry about the vacancy in this case is C_s rather than C_{3v}. In the analysis of the Raman data, we have chosen an orthogonal coordinate system such that y is parallel to the line connecting the 6c sites in the conducting plane , and z is parallel to the crystallographic c-axis. The mirror plane of the C_s site in this system is the yz plane.

We have analyzed the Raman data based on the localized normal modes of a defect cluster consisting of a vacant site surrounded by three cations (Fig. 5). As noted above, it was found from our model calculations that a cluster of C_s symmetry is the most stable configuration at temperatures above 0 K. The irreducible representations of the modes of a C_s cluster are given by $\Gamma = 5A' + 4A''$. These include modes which can be described by internal and external normal coordinates of the cluster. Because there are three equivalent orientations of the cluster related by three-fold rotations about a 6c site, the change in the orientation of the coordinate axes on rotation about the three-fold axis must be taken into account in order to determine the polarization of the light scattered by the A' and A" modes. If α represents

the scattering tensor at one site, then the scattering tensor at the other sites is given by $\alpha' = R\alpha R^t$, where R is a transformation matrix for rotation by $\pi/3$ or $2\pi/3$ about the z axis. Here, α corresponds to $\alpha(A')$ or $\alpha(A'')$ of the C_s point group. Since the Raman intensity for the (ij) polarization is proportional to $(\alpha'_{ij})^2$, the total scattering from the clusters in all three orientations is proportional to $(\alpha'_{ij})^2_T$, where $(\alpha'_{ij})^2_T = (\alpha'_{ij})^2_1 + (\alpha'_{ij})^2_2 + (\alpha'_{ij})^2_3$.

These terms represent the elements of the transformed tensors, $\alpha'(A')$ and $\alpha'(A'')$. Details of this calculation are given elsewhere [3].

The effect of summing over the three orientations is that both $\alpha(A')$ and $\alpha(A'')$ contribute to the scattering in each of these polarizations, so that all Raman active modes are allowed in (a'a'), (a'a), and (ca) polarizations. This accounts for the fact that the same Raman peaks were observed in all three of these polarizations. On the other hand, the calculations also show that it is possible to distinguish between the A' and A" modes, since A' modes will give rise to Raman peaks in (cc) polarization, while the A" modes are forbidden in this polarization. This result was used to assign the bands listed in Table II to either A' or A" modes: Those bands which were observed in (cc) polarization were assigned to A' modes, while the remaining peaks were assigned to A" modes.

The frequencies of several vibrational modes of the defect cluster were calculated from our model of Naβ". The atomic displacements and corresponding frequencies of two of these modes are given in Fig. 6. The mode of Fig. 6(a) is a symmetric vibration of A' symmetry, and the calculated frequency of 100 cm^{-1} agrees well with the frequency of a band observed at 93 cm^{-1} and assigned to an A' mode. The mode illustrated in Fig. 6(b) has A" symmetry since it is asymmetric with respect to reflection in the vertical (σ_{yz}) plane. The calculated frequency of 30 cm^{-1} is close to a Raman band observed at 33 cm^{-1} and attributed to an A" mode.

It can be seen in Fig. 6(b) that extending the atomic displacement vectors of the two atoms which move along the lines connecting the 6c sites will lead to a jump diffusion step. We therefore associate the 33 cm^{-1} (1.0×10^{12} Hz) Raman band with the attempt frequency for diffusion of Na^+ ions in beta"-alumina.

Calculations of the frequencies for the vibrational modes of defect clusters in K- or Agβ" have not yet been attempted. Because force constant changes often occur with changes in the type of mobile cation, assignments of the Kβ" and Agβ" Raman spectra based on a simple reduced mass scaling of the Naβ" frequencies are not reliable. This point is underscored by comparing the observed Li^+ frequencies (Table II) with those calculated from the observed Na^+ frequencies.

CONDUCTION MECHANISM

Ion transport in beta"-alumina occurs by means of a vacancy mechanism [12], and we have made some preliminary model calculations of the details of this mechanism. Starting with the minimum energy configuration shown in Fig. 5, one of the three Na^+ ions neighboring a vacancy was moved in small steps toward the vacant site. Nearby Na^+ ions were allowed to relax after each step in order to minimize the potential energy. This process was continued until the ion and vacancy exchanged sites. The activation energy, taken to be the difference between the potential energy at the saddle point and the potential energy at the equilibrium configuration, was calculated to be about 0.02 eV. Although the calculated activation energy is much smaller than the experimental value of 0.18 eV (Fig. 1), it is consistent with the low attempt frequency observed at 33 cm^{-1}. Assuming a random walk model for a two-dimensional jump diffusion process, the pre-exponential factor was calculated to be $\sigma_0 = 39.6\ \nu_0$, where ν_0 (cm^{-1}) is the attempt frequency.

The Arrehenius equation for the graph in Fig. 1 is given by

$$\sigma T = 9.29 \times 10^3 \exp(-0.28/kT)\ (\Omega\text{-cm})^{-1}\ K, \quad (1)$$

while the expression derived from the model calculation is

$$\sigma T = 1.19 \times 10^3 \exp(-E_a/kT)\ (\Omega\text{-cm})^{-1}\ K, \quad (2)$$

using the calculated attempt frequency, $\nu_0 = 30\ cm^{-1}$. Not only is the calculated activation energy (0.02 eV) an order of magnitude smaller than the measured value, but the calculated pre-exponential factor is likewise nearly an order of magnitude smaller than the experimental result. The disagreement between experiment and theory can be resolved by

assuming a temperature dependent activation energy:

$$E_a = 0.18 - 1.77 \times 10^{-4} T \text{ eV} . \qquad (3)$$

The coefficient of T was calculated by requiring that Eq. (1) yield the same values of σT as given by Eq. (2). Additional terms of order T^2 or higher in Eq. (3) could explain the curvature in the log σT vs. $1/T$ graph of Weber's data [1]. The origin of the temperature dependence of E_a is not known at the present time, but it does seem to be required in order that the low attempt frequency be associated with high ionic conductivity.

ACKNOWLEDGMENTS

We thank W. R. Busing and Debra Schwinn for assistance in data collection for the crystal structure determination.

REFERENCES

1. J. T. Kummer, Prog. in Solid State Chem. 7, 141 (1972).

2. W. E. Brundage and J. B. Bates, Solid State Ann. Prog. Report (ORNL-5486), 194 (1978).

3. W. L. Roth, F. Reidinger, and S. LaPlaca in "Superionic Conductors," G. D. Mahan and W. L. Roth, eds. (Plenum Press, New York, 1976), p. 233.

4. M. Bettman and C. R. Peters, J. Phys. Chem. 73, 1774 (1969)

5. F. Reidinger, S. LaPlaca, and W. L. Roth, private communication of work in progress.

6. S. J. Allen, Jr., A. S. Cooper, R. DeRosa, J. P. Remeika, and S. K. Vlasi, Phys. Rev. B 17, 4031 (1978).

7. P. Coppens and W. C. Hamilton, Acta Cryst. A 26, 1 (1970).

8. G. C. Farrington and J. L. Briant, private communications.

9. T. Kaneda, J. B. Bates, and J. C. Wang, Solid State Commun. 28, 469 (1978).

10. R. Frech and J. B. Bates, Spectrochim. Acta (in press, 1979).

11. J. C. Wang, M. Gaffari, and S. Choi, J. Chem. Phys. 63, 772 (1975).

12. J. C. Wang, J. B. Bates, T. Kaneda, and H. Engstrom, Bull. Am. Phys. Soc. 24, 433 (1979).

13. J. B. Bates, T. Kaneda, W. E. Brundage, J. C. Wang and H. Engstrom, Solid State Commun., submitted for publication, 1979.

TABLE I. STRUCTURAL DATA FOR Ag-BETA"-ALUMINA

Unit cell parameters:[a] $a_0 = 5.6295(15)$ Å
$c_0 = 33.4210(10)$ Å

Composition: 0.80 Ag_2O · 0.66 MgO · 5 Al_2O_3

0.80 Ag^+ on 6c 0.34 Mg^{2+} on Al(2) sites

Anisotropic Thermal Parameters[b,c] (Å^2)

	U_{11}	U_{22}	U_{33}
Ag^+	0.0630	0.0630	0.0275
Na^+	0.1245	0.3871	0.3042

(a) Parameters for triply primitive hexagonal unit cell.

(b) From the temperature factor expression, $\exp[-2\pi^2(h^2a^{*2}U_{11} + k^2b^{*2}U_{22} + l^2c^{*2}U_{33} + 2hka^*b^*U_{12} + 2hla^*c^*U_{13} + 2klb^*c^*U_{23})]$.

(c) Sodium parameters from ref. [5].

TABLE II. FREQUENCIES OF RAMAN BANDS ASSIGNED TO VIBRATIONS OF MOBILE CATIONS IN BETA"-ALUMINAS

Frequencies (cm^{-1})[a,b]

^6Li	^7Li	Na	K	Ag
445(A')	437(A')	220(A')		
409(A')	397(A')	170(A')		
		142(A')	90(A")	90(A')
		93(A')	78(A")	50(A')
		85(A")	73(A")	31(A')
		32(A")		22(A')

(a) Frequencies for Na, K, and Agβ"-alumina observed at 15 K. Frequencies for ^6Li- and ^7Liβ" observed at 300 K.

(b) Assignment to A' or A" species of C_s point group based on discussion in text.

FIGURE CAPTIONS

Fig. 1. Ionic conductivity of a Na beta"-alumina single crystal as a function of temperature. The solid line is the result of a least-squares fit of the conductivity data to an Arrehenius equation.

Fig. 2. Stereoscopic drawing of the central two-thirds of two adjacent hexagonal unit cells of Ag beta"-alumina. The small circles labelled A represent the Ag^{+} ions. The other small and large circles with numerals represent the various crystallographically distinct Al^{3+} and O^{2-} ions, respectively.

Fig. 3. Comparison of the Raman scattering from Naβ"-alumina and Naβ-alumina measured at 15 K. (a) Spectrum of Naβ" for (ca) polarization. (b) Spectrum of Naβ for (a'a) polarization.

Fig. 4. Raman spectra of Na, K, and Agβ"-alumina for (a'a') polarization measured at 15 K.

Fig. 5. Calculated positions of Na^{+} ions near the plane defined by the O^{2-} ions in Naβ"-alumina. Small solid circle denotes vacant cation site.

Fig. 6. Calculated frequencies and schematic atomic displacements for several vibrational modes of the defect cluster in Naβ"-alumina.

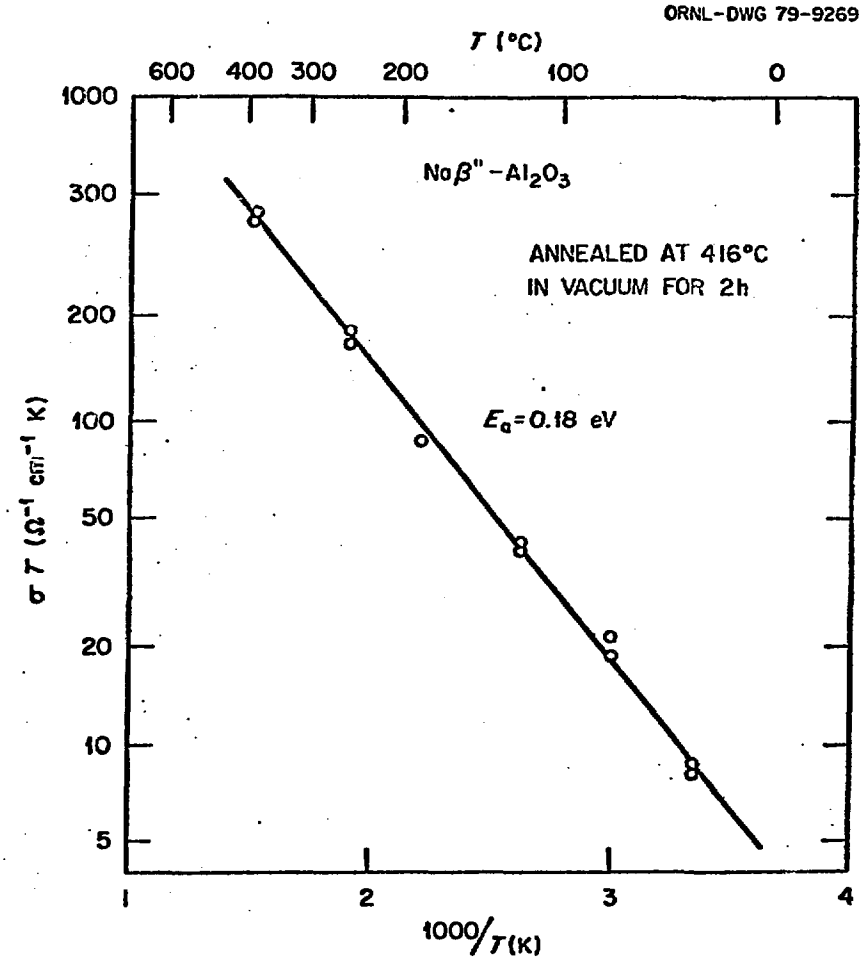
ORNL-DWG 79-9269
T (°C)
600
400
300
200
100
0
1000
300
200
100
50
20
10
5
Naβ"-Al2O3
ANNEALED AT 416°C
IN VACUUM FOR 2h
Ea=0.18 eV
σ T (Ω-1 cm-1 K)
1
2
3
4
1000/T(K)

Fig. 1

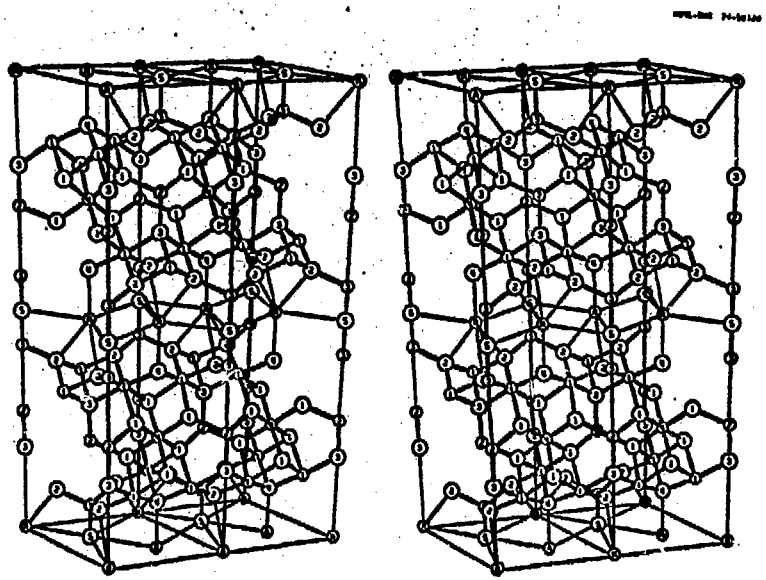

Fig. 2

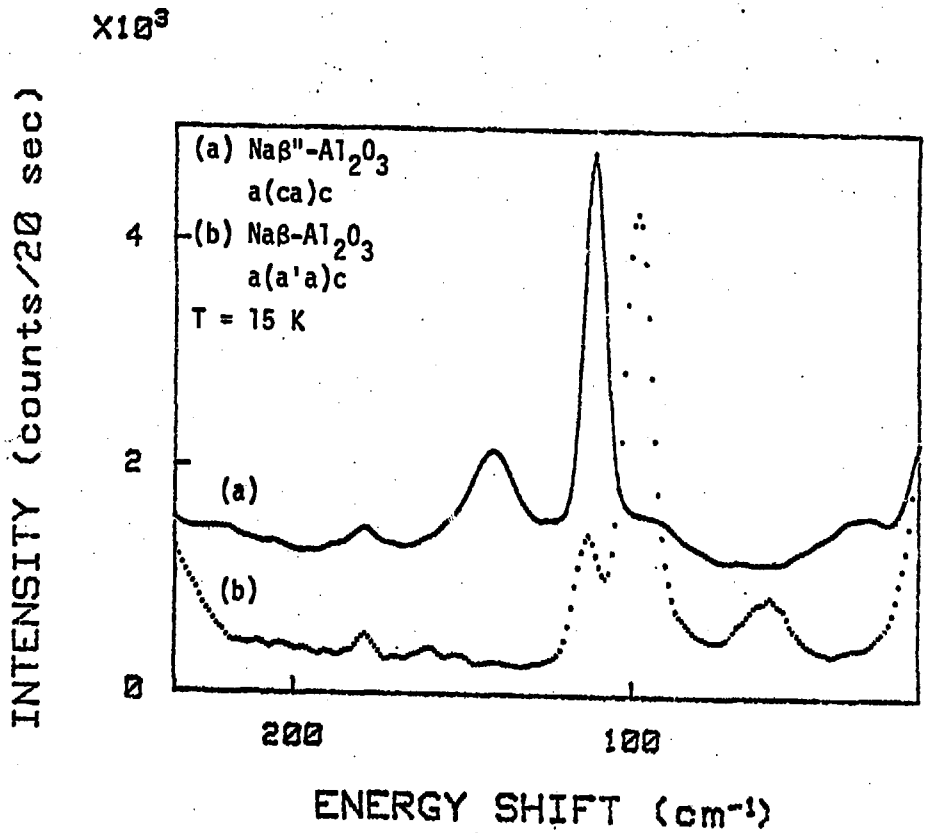
X10³
INTENSITY (counts/20 sec)
4
2
0
(a) Naβ"-Al2O3
a(ca)c
(b) Naβ-Al2O3
a(a'a)c
T = 15 K
(a)
(b)
200
100
ENERGY SHIFT (cm⁻¹)

Fig. 3

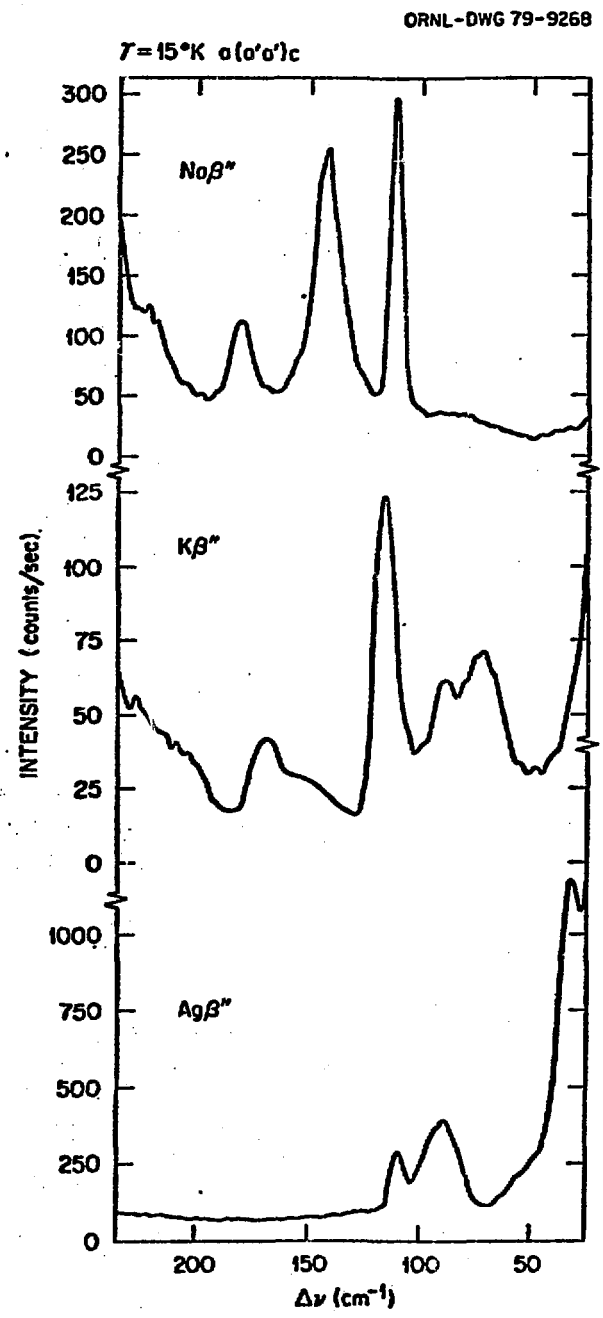
ORNL-DWG 79-9268
T = 15°K a(a'a')c
Naβ"
Kβ"
Agβ"
INTENSITY (counts/sec)
300
250
200
150
100
50
0
125
100
75
50
25
0
1000
750
500
250
0
200
150
100
50
Δν (cm⁻¹)

Fig. 4

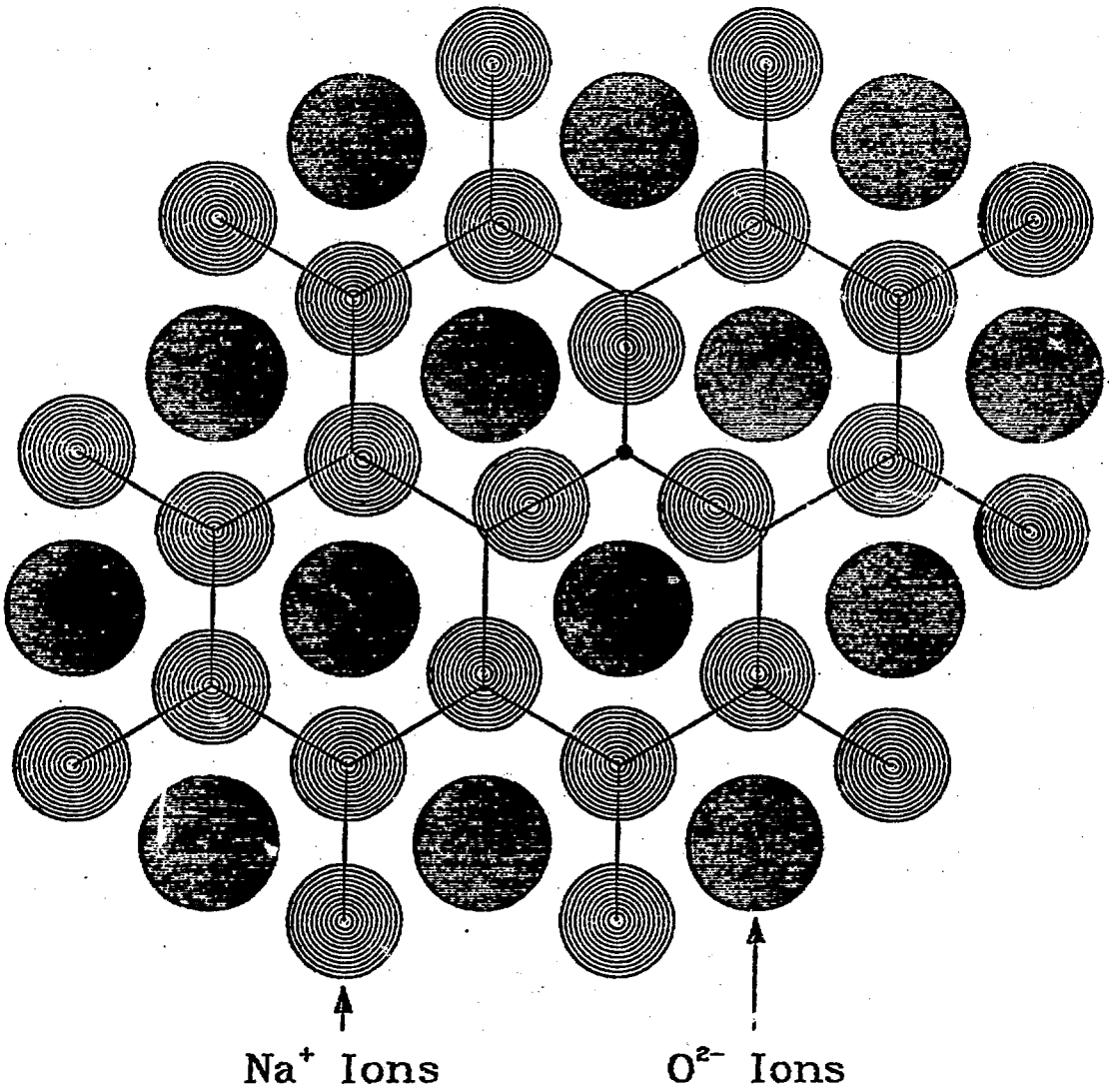

Fig. 5

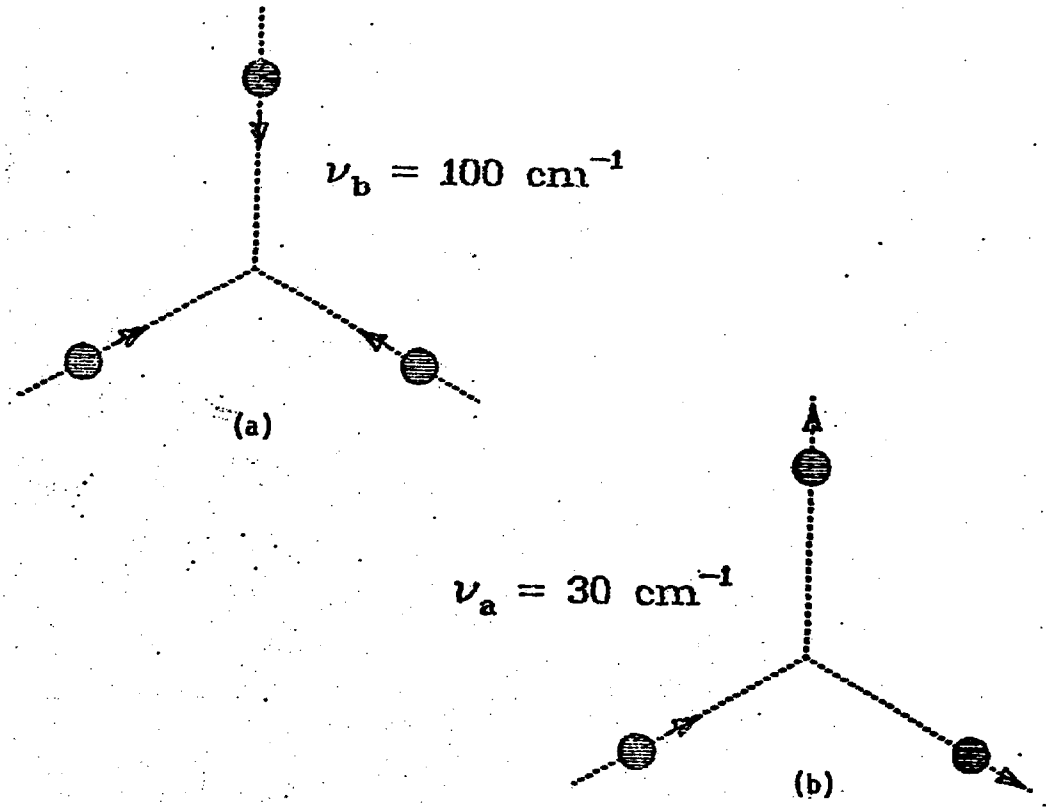

Fig. 6